CrossMark

ORIGINAL PAPER

Evaluation of rainfall simulations over West Africa in dynamically downscaled CMIP5 global circulation models

A.A Akinsanola[1,2] · V.O Ajayi[2] · A.T Adejare[2] · O.E Adeyeri[2] · I.E Gbode[2] ·
K.O Ogunjobi[2] · G Nikulin[3] · A.T. Abolude[1]

Abstract This study presents evaluation of the ability of Rossby Centre Regional Climate Model (RCA4) driven by nine global circulation models (GCMs), to skilfully reproduce the key features of rainfall climatology over West Africa for the period of 1980-2005. The seasonal climatology and annual cycle of the RCA4 simulations were assessed over three homogenous subregions of West Africa (Guinea coast, Savannah, and Sahel) and evaluated using observed precipitation data from the Global Precipitation Climatology Project (GPCP). Furthermore, the model output was evaluated using a wide range of statistical measures. The interseasonal and interannual variability of the RCA4 were further assessed over the subregions and the whole of the West Africa domain. Results indicate that the RCA4 captures the spatial and interseasonal rainfall pattern adequately but exhibits a weak performance over the Guinea coast. Findings from the interannual rainfall variability indicate that the model performance is better over the larger West Africa domain than the subregions. The largest difference across the RCA4 simulated annual rainfall was found in the Sahel. Result from the Mann–Kendall test showed no significant trend for the 1980–2005 period in annual rainfall either in GPCP observation data or in the model simulations over West Africa. In many aspects, the RCA4 simulation driven by the HadGEM2-ES perform best

over the region. The use of the multimodel ensemble mean has resulted to the improved representation of rainfall characteristics over the study domain.

1 Introduction

The West Africa is one of the most populated regions of the world and is highly vulnerable to the adverse effects of weather and climate variability (IPCC 2007). This vulnerability is as a result of its low adaptive capacity to observed changes in climate (Omotosho and Abiodun 2007). Scientists within the region have projected that the changes in climate may result to severe impacts on diverse key sectors of the economy such as hydroelectric power generation, agriculture, water management, and health. Therefore, regional and local information about climate change is needed by multiple applications in the field of resource management, impact assessment, and policy planning (Fuhrer et al. 2014; Stoffel et al. 2014). Downscaling a global circulation model (GCM) dynamically with a regional climate model (RCM) is one of the ways to derive this information (Rummukainen 2010). RCMs are frequently used because of their consistent representation of physical processes at a very high resolution, and also, they show quite realistic climate signals when compared to observations (Christensen et al. 1998; Giorgi et al. 2009; Feser et al. 2011). The crucial role that RCMs play in the simulation of such physical processes emphasizes the need to characterize the strengths, weaknesses, and uncertainties in them (Kim et al. 2014; Xue et al. 2014). Many GCMs have been downscaled by RCMs in the framework of large coordinated efforts in order to assess their potentials for regional climate projection studies (Christensen and Christensen 2007; van der Linden and Mitchell 2009; Giorgi et al. 2009; Jacob and Coauthors 2014). It is important to state that these past efforts provided

✉ A.A Akinsanola
   mictomi@yahoo.com

1 School of Energy and Environment, City University of Hong Kong, Kowloon Tong, Hong Kong SAR, China

2 Department of Meteorology and Climate Science, Federal University of Technology Akure, Akure, Nigeria

3 Swedish Meteorological and Hydrological Institute, Norrköping, Sweden

Springer

a new opportunity for the intercomparison of different models, initial and lateral boundary conditions, parameterization schemes, and grid resolutions (Jacob et al. 2007; Nikulin et al. 2012; Gbobaniyi et al. 2013; Sylla et al. 2013; Akinsanola et al. 2015; Klutse et al. 2015).

The Coordinated Regional Climate Downscaling Experiment (CORDEX) is an initiative sponsored to provide a platform for a joint evaluation of model performance, along with a solid scientific basis for impact assessments and adaptation studies in the area of climate change by making high-resolution climate projections readily available to users (Giorgi et al. 2009). The experiment is the first effort that focuses on the whole of Africa and furthermore treats it as a priority domain (Nikulin et al. 2012). CORDEX consisted of two phases: in the first phase, downscaling centers were asked to downscale a reference/verification period using Era Interim reanalysis dataset from the European Centre for Medium-Range Weather Forecasts (ECMWF), (Dee and Coauthors 2011) and in the second phase, ensembles of historical and future climate projections at high resolution was done at regional scale, by downscaling the GCMs participating in the Coupled Model Intercomparison Project Phase 5 (CMIP5) (Taylor et al. 2012).

Published work within CORDEX-Africa climate framework especially for precipitation assessment which is also the focus of this study indicates strengths and weakness in state-of-the-art modelling tools. The first phase of the present-day CORDEX-Africa simulations using ERA-Interim reanalysis at the boundaries has been analyzed in detail (Druyan et al. 2010; Paeth et al. 2011; Nikulin et al. 2012; Diallo et al. 2012, 2013; Laprise et al. 2013; Gbobaniyi et al. 2013; Sylla et al. 2013; Kim et al. 2014; Akinsanola et al. 2015; Klutse et al. 2015), where they focused mostly on precipitation climatology. The RCMs were found to accurately simulate the seasonal mean and annual cycle of precipitation, although the performance of the individual RCMs varies to a very large extent from region to region and from one season to another. Also, they reported differently that multimodel ensemble mean outperforms any individual RCM simulation. Christensen et al. (1998) has revealed that RCMs are unable to "correct" systematic errors in large-scale circulation from driving data. Presently, only few research studies have been carried out on the evaluation of West Africa rainfall characteristics and its representation in the second phase of the CORDEX-Africa. Therefore, this study is aimed at evaluating the performance of the Rossby Centre Regional Climate Model–RCA4 driven by nine CMIP5 GCMs, to accurately replicate the historical rainfall characteristics over West Africa.

2 Study area

The study area of this research is West Africa. The region as shown in Fig. 1 broadly lies between longitude 20° W and 20°
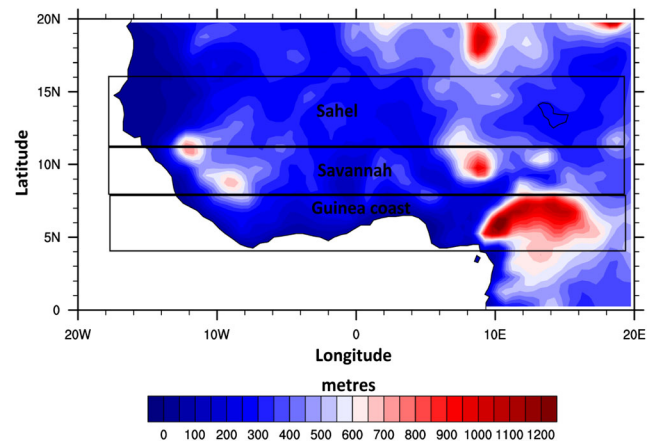

Fig. 1 Study domain showing West Africa topography and the regions designated as Guinea coast, Savanna, and Sahel zones in the study (adapted from Abiodun et al. (2012))

E and latitude 0° and 20° N. Geographically, the Gulf of Guinea is the Southern boundary, while to the North is the Northern boundary of Mauritania, Mali, and Niger. Its Eastern and Western limits are, respectively, to Mount Cameroun and the Atlantic Ocean as described in Akinsanola et al. (2015). Adopting the classification of Omotosho and Abiodun (2007) and Abiodun et al. (2012), West Africa is divided into three climatic zones, namely, Guinea Coast (4°–8° N), Savannah (8°–11° N), and Sahel (11°–16° N). The Guinea coast represents the southern boundary to the Atlantic Ocean which is characterized by the sub-humid climate with an average annual rainfall between 1250 and 1500 mm. The Savannah zone is a semi-arid zone with an average annual rainfall between 750 and 1250 mm. The Sahel zone covers the northern boundary of Mauritania, Mali, and Niger characterized by a single rainfall peak but short rainy season (June–September) with an annual rainfall of about 750 mm. The variability in the climate of West Africa is also greatly influenced by topography (Akinsanola et al. 2015). Some of the most important plateaus are Fouta Djallon, Jos Plateau, and the Cameroon Highland as indicated by the topographic details highlight in Fig. 1.

3 Data and methods

Nine RCA4 simulations driven by CMIP5 GCMs were analyzed and intercompared. These GCMs were dynamically downscaled by the latest version of the Rossby Centre Regional Climate Model (RCA4) developed by the Swedish Meteorological and Hydrological Institute (SMHI) under the CORDEX framework (Samuelsson et al. 2011; Strandberg et al. 2014; Kjellström et al. 2014). Presently, the improvement of energy flux parameterization within the RCA4 dynamic core makes it more physically consistent, as well as relative reduction of compensating errors with improved

representation of the diurnal temperature cycle. It is important to state that the explicit treatment of aerosol changes is still unaddressed as described in details by Samuelsson et al. (2011). The historical simulation was integrated over the CORDEX Africa domain at a spatial resolution of 0.44° × 0.44° (~50 km × 50 km) for the time period of 1951–2005. In this study, an evaluation of the historical run of the RCA4 simulations (see Table 1) was performed over West Africa, and a multimodel ensemble mean of the RCA4 simulations referred therein as "Ensmean" was also evaluated. All the simulation datasets were obtained from the Climate Systems Analysis Group (CSAG) of the University of Cape Town, Cape Town, South Africa, and also available on the Earth System Grid Federation (ESGF) under the CORDEX project.

The Global Precipitation Climatology Project (GPCP) product version 2.3 precipitation dataset (Adler et al. 2003) with a spatial resolution of 2.5° by 2.5° was used to compare and validate the RCA4 simulations. Sylla et al. (2013) examined a number of rainfall products available over Africa and found that they exhibit substantial systematic differences in mean rainfall. However, they reported that the GPCP which is satellite derived is more consistent with gauge-based observations than the other rainfall products over Africa.

Since the model and GPCP datasets used in this study have different spatial and temporal resolutions, it is important to state that all datasets were re-gridded to a spatial resolution of 50 km (~0.44°) using bilinear interpolation as in Nikulin et al. (2012) for easy comparison. Also to address the uniformity in the temporal span of all the datasets, the rainfall data were aggregated into monthly means over the period of 1980–2005. Two seasons were selected to compare and study the rainfall estimates in detail: the dry season (December–February) and the summer monsoon season (June–September). A comparison was performed for the three main subregions over West Africa earlier illustrated in Fig. 1. For each subregion and season, the comparison was done in two ways, mean climatological and statistical description. The mean climatological description is presented by showing the spatial rainfall pattern, latitude-time cross section, interseasonal and interannual variability.

Furthermore, the statistical analysis includes three detailed statistical approaches. Firstly, the fit to different theoretical distributions was investigated using cumulative density function (CDF). A cumulative distribution $F(x)$ can be defined as the proportion of observations lying below a certain value x. The cumulative distribution for all the models simulation runs is compared with observed data. Secondly, a trend detection analysis was performed using Mann-Kendall (MK) test. The MK test have been used in earlier studies to detect trend in rainfall data (Mann 1945; Kendall 1975; de la Casa and Nasello 2010, 2012; Krishnakumar et al. 2009; Subash et al. 2011; Akinsanola and Ogunjobi 2015).

Test statistic S is defined as follows:

$$S = \sum_{i=1}^{n-1} \sum_{j=i+1}^{n} sgn\left(x_j - x_i\right)$$

where x_j is the sequential data value, n is the length of the dataset, and

$$sgn(y) = \begin{cases} 1 \dots & \text{if}(y > 0) \\ 0 \dots & \text{if}(y = 0) \\ -1 \dots & \text{if}(y < 0) \end{cases}$$

It has been documented that when $n \geq 8$, the statistic S is approximately normally distributed with the mean $E(S) = 0$ and variance as

$$V(S) = \frac{n(n-1)(2n+5) - \sum_{i=1}^{m-1} t_i(t_i-1)(2t_i+5)}{18}$$

Table 1 Description of the CMIP5 global climate models (GCMs) downscaled by RCA4

Institute	Country	GCM name	Short name
Canadian Centre of Climate Modelling and Analysis	Canada	CCCma-CanESM2	CanESM2
NOAA Geophysical Fluid Dynamics laboratory	USA	NOAA-GFDL-GFDL-ESM2M	GFDL-ESM2M
Consortium of European research institution and researchers	Europe	ICHEC-EC-EARTH	EC-EARTH
The Norwegian Climate Center	Norway	NCC-NorESM1-M	NorESM1-M
Met Office Hadley Centre	UK	MOHC-HadGEM2-ES	HadGEM2-ES
Max-Planck-Institut für Meteorologie (Max Planck Institute for Meteorology)	Germany	MPI-M-MPI-ESM-LR	MPI-ESM-LR
CNRM-CERFACS: Centre National de Recherches Météorologiques—Groupe d'études de l'Atmosphère Météorologique et Centre Européen de Recherche et de Formation Avancée	France	CNRM-CERAFACS-CNRMCM5	CNRM-CM5
National Institute for Environmental Studies, and Japan Agency for Marine-Earth Science and Technology	Japan	MIROC-MIROC5	MIROC5
Institut Pierre-Simon Laplace	France	IPSL-IPSL-CM5A-MR	IPSL-CM5A-MR

where m is the number of tied groups and t_i is the size of the ith tied group. The standardized test statistic Z is computed by

$$Z_{MK} = \begin{cases} \dfrac{S-1}{\sqrt{\text{Var}(S)}} & \text{when } S > 0 \\ 0 \quad \cdots & \text{when } S = 0 \\ \dfrac{S+1}{\sqrt{\text{Var}(S)}} & \text{when } S < 0 \end{cases}$$

In addition, the model performance was further investigated using the following statistical indices: mean bias error (MBE), mean gross error (MGE), root mean squared error (RMSE) and correlation coefficient (r). Lastly, in order to assess the consistency in model simulations, the study further examined the model's ability to capture the observed deviation in annual rainfall amounts. A comparison of rainfall anomaly (Ra) of the RCA4 simulations and observation is done using the equation below.

$$R_a = \frac{Rt - \overline{R}}{\overline{R}}$$

where Rt is the average rainfall amount of a certain year (t) and $\overline{R}$ is the long-term mean rainfall.

4 Results and discussion

4.1 Mean climatology

Before evaluating and intercomparing the characteristics of monthly rainfall over West Africa simulated by RC4, it is important to assess the mean climatology. The spatial distribution of mean December-January-February (DJF) rainfall climatology (1980–2005) over West Africa is shown in Fig. 2a for GPCP and each of the RCA4 simulations (Fig. 2b–j) along with their multimodel ensemble mean (Fig. 2k). The RCA4 simulated rainfall climatologies were overall consistent with GPCP observation; major part of the West African domain was having rainfall below 1 mm, while the highest rainfall amount was observed in the Guinea coast. The spatial distribution of mean June-July-August-September (JJAS) rainfall climatology is shown is Fig. 3. The mean annual distribution of rainfall in West Africa is generally zonal with the rainfall amount decreasing from coast to inland. The heaviest rainfall occurs in the southwest and southeast of West Africa as observed also by (Udo 1978; Nicholson 2003, Afiesimama et al. 2006; Gbobaniyi et al. 2013; Akinsanola et al. 2016). The GPCP dataset depicts two rainfall maxima. The rainfall maximum observed over the coastal areas of the Guinean Highlands has a value of 13 mm/day. Similarly, another zone of maximum rainfall was observed over the Cameroonian highland with a value of about 9 mm/day. The

RCA4 simulations and the multimodel ensemble mean were consistent in capturing the observed features in GPCP. However, bias varies substantially in the model in terms of magnitude and spatial extent. The RCA4 simulations driven by IPSL-CM5A-MR, MIROC5, HadGEM2-ES, and GFDL-ESM2M consistently overestimated the observed orographic rainfall around the Guinean Highlands. Difficulty in simulating rainfall accurately in model data especially over the monsoon regions were also observed by Xue et al. (2010), Ruti et al. (2011), Nikulin et al. (2012), and Gbobaniyi et al. (2013). The reason for the higher rainfall simulated by the RCA4 over these regions may be connected to the low-level convergence (Afiesimama et al. 2006) and also, RCA4 inability to accurately simulate the interactions between deep convection, orography induced rainfall and West African Monsoon elements (Sylla et al. 2011). Despite these discrepancies, the RCA4 simulations were able to capture these regions of higher rainfall. Ultimately, the Ensmean outperformed the individual members in capturing the observed features both spatially and in magnitude.

The northward propagation and gradual retreat of rainfall have been identified as one of the most crucial feature of the West African Monsoon (Le Barb e et al. 2002; Sultan and Janicot 2000; Nikulin et al. 2012; Akinsanola et al. 2015). Figure 4 shows the latitude–time cross section of mean monthly rainfall over the period 1980–2005 averaged along 10° W–10° E for the GPCP observation and the RCA4 simulations. The GPCP observation exhibits a first major quasi-stationary monsoon front south of latitude 6° N in the month of May, and this corresponds to the monsoon onset over the Guinea coast. The high-intensity rainband jumps toward the Sahel subregion and the maximum rainfall appears north of latitude 9° N in August. This month of maximum rainfall over the Sahel correspond to the period of little dry season over the Guinea coast. The high amounts of rainfall, of more than 7 mm/day, end around October after the monsoon retreats toward the Guinea coast. The GPCP observation revealed that the seasonal advance and retreat of the summer monsoon rainfall behaves in a stepwise rather than a continuous manner. Majority of the RCA4 simulations fairly reproduce the maximum rainfall in the Sahel subregion occurring in August with differing magnitude. The model simulations failed to reproduce the two rainfall peaks, and also, the little dry season in the Guinea coast except for HadGEM2-ES which agrees reasonably well with the GPCP observation. All the simulations except that of HadGEM2-ES and MIROC5 failed to capture the asymmetric behavior of the rainfall amount between the onset and retreat periods as seen in the GPCP observations.

The annual cycle of the model simulations and their multimodel ensemble mean relative to GPCP is investigated over the three homogeneous subregions and the entire West Africa domain is presented in Fig. 5. Over the Guinea coast, GPCP exhibits two peaks of rainfall, a primary maximum in
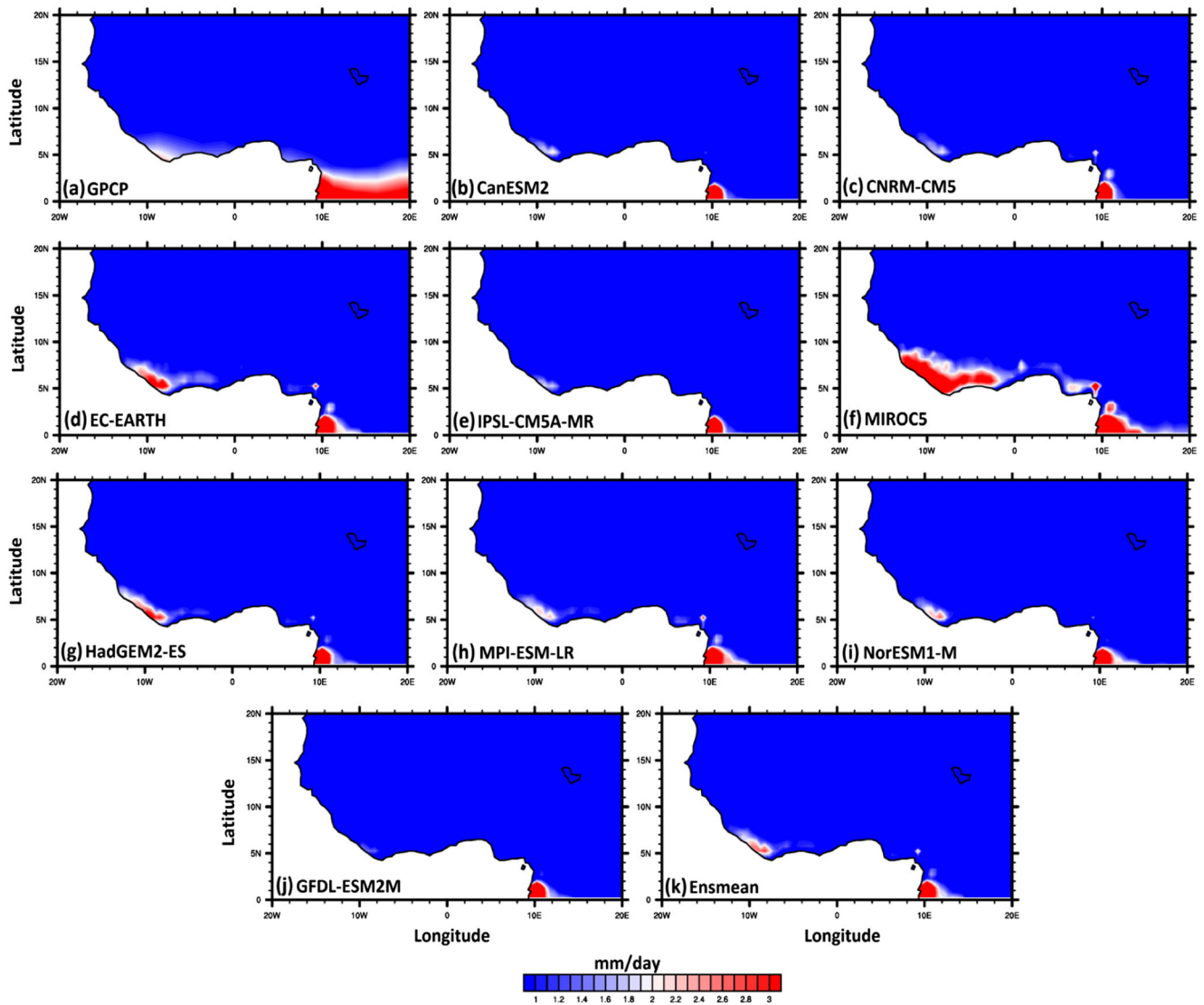
Fig. 2 Spatial distribution of mean monthly DJF rainfall (mm/day) over West Africa from 1980 to 2005 for **a** GPCP, **b** CanESM2, **c** CNRM-CM5, **d** EC-EARTH, **e** IPSL-CM5A-MR, **f** MIROC5, **g** HadGEM2-ES, **h** MPI-ESM-LR, **i** NorESM1-M, **j**) GFDL-ESM2M, and **k** Ensmean

June, and a secondary in September. Also observed is a relative mid-summer low (minimum) in August as the seasonal monsoon rain band propagates in the north–south direction over the Guinea coast. Only two RCA4 members (i.e., HadGEM2-ES and CanESM2) were consistent with GPCP in capturing the observed two peaks of rainfall. Majority of the simulations overestimated the observed rainfall amount and distinctively failed to capture the little dry season (LDS) in August. In the Savannah, the length of raining season extends from May to October, with rainfall exhibiting a unimodal pattern, having its peak in the month of August. The RCA4 members replicate this trend considerably well as seen in Fig. 5b, although IPSL-CM5A-MR-, GFDL-ESM2M-, HadGEM2-ES-, and MIROC5-driven simulations all overestimated the peak rainfall. In the Sahel, as observed by GPCP, the length of rainy season is not up to 4 months (i.e. between July and September), with August having the highest

rainfall amount. The RCA4 simulations were consistent in reproducing the rainfall pattern over this region. Simulations driven by EC-EARTH and NorESM1-M captured an early peak in May. Over the entire West African domain, a smoother annual cycle with obvious shift of peak to September was observed in most of the RCA4 simulations and their multimodel ensemble mean. These observations illustrate the importance of clearly defined and area-averaged climatic parameters over different climatically homogenous subregions.

4.2 Interannual variability

The annual relative change, which is a measure of the interannual variability, poses the need to assess the magnitude of the RCA4 deviation from the observation. Figure 6 presents the percentage differences of the model simulations considered and the multimodel ensemble mean from the
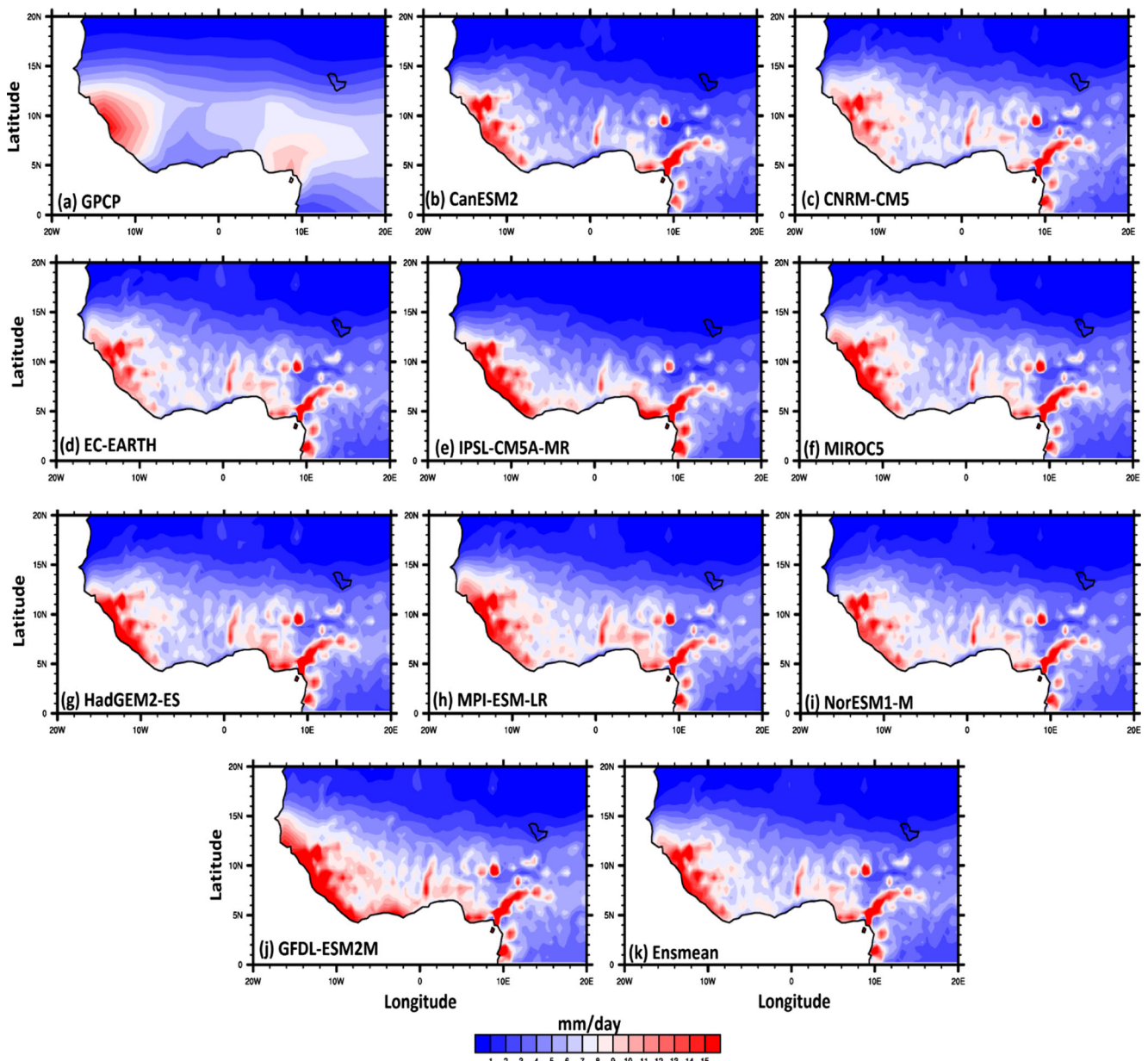
Fig. 3 Same as Fig. 2 but for JJAS

observation over three homogenous zones and the entire West Africa. Over the Guinea coast, seven of the RCA4 simulations overestimate the rainfall by about 10–40%, with the smallest bias occuring in the multimodel ensemble mean and NorESM1-M. The MIROC5-driven simulation recorded the highest positive bias of about 40% out of the entire simulations. Also, the RCA4 simulations driven by CNRM-CM5, EC-EARTH, and CanESM2 underestimated the rainfall amount over the year. Over the Savannah, the multimodel ensemble mean recorded lowest percentage difference while the HadGEM2-ES and CanESM2 had the highest percentage of overestimation and underestimation, respectively. In the Sahel, the observed percentage rainfall bias in the RCA4 simulations are very large because of the fact that the annual rainfall received over the subregion is very low. Both the Ensmean and CNRM-CM5 recorded the lowest percentage difference while the GFDL-ESM2M and IPSL-CM5A-MR recorded the highest percentage of overestimation and underestimation, respectively. Over the entire West Africa domain, the Ensmean recorded the lowest percentage difference. All the RCA4 simulations were consistent in capturing the interannual variability of rainfall amount with differing level of accuracy. The lowest percentage difference in the RCA4 performance was observed over a bigger domain of West Africa. The Ensmean consistently outperforms the individual model simulations in capturing the amount of annual rainfall in all the subregions and the whole West Africa domain.
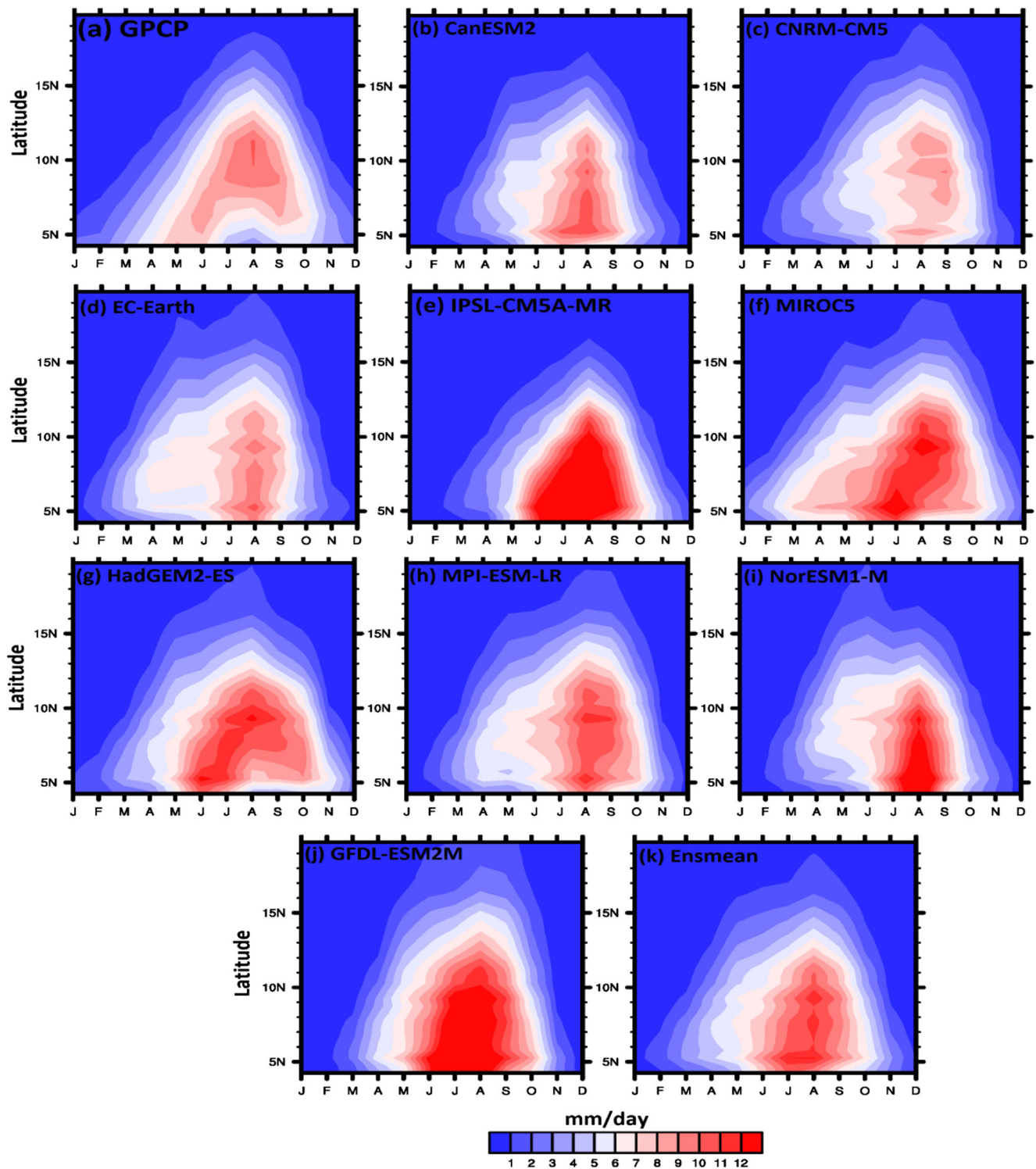
Fig. 4 Latitude-time cross section of monthly mean rainfall (mm/day) averaged from 10° W to 10° E for **a** GPCP, **b** CanESM2, **c** CNRM-CM5, **d** EC-EARTH, **e** IPSL-CM5A-MR, **f** MIROC5, **g** HadGEM2-ES, **h** MPI-ESM-LR, **i** NorESM1-M, **j** GFDL-ESM2M, and **k** Ensmean for the period 1980–2005

4.3 Annual rainfall anomaly

Following the classification of McKee et al. (1993), annual rainfall anomaly Ra may be used to categorize normal, dry, and wet years based on the following definitions; the normal years ($-0.99 < Ra < 0.99$), dry years ($Ra < -0.99$), and wet years ($Ra > 0.99$). This classification was then used to evaluate the ability of the RCA4 simulations to accurately identify the

Fig. 5 Monthly mean variation of area-averaged rainfall (mm/day) over the **a** Guinea coast, **b** Savannah, **c** Sahel subregions, and **d** the entire West Africa for GPCP observation, each of the RCA4 simulations and their multimodel ensemble mean for the period of 1980–2005
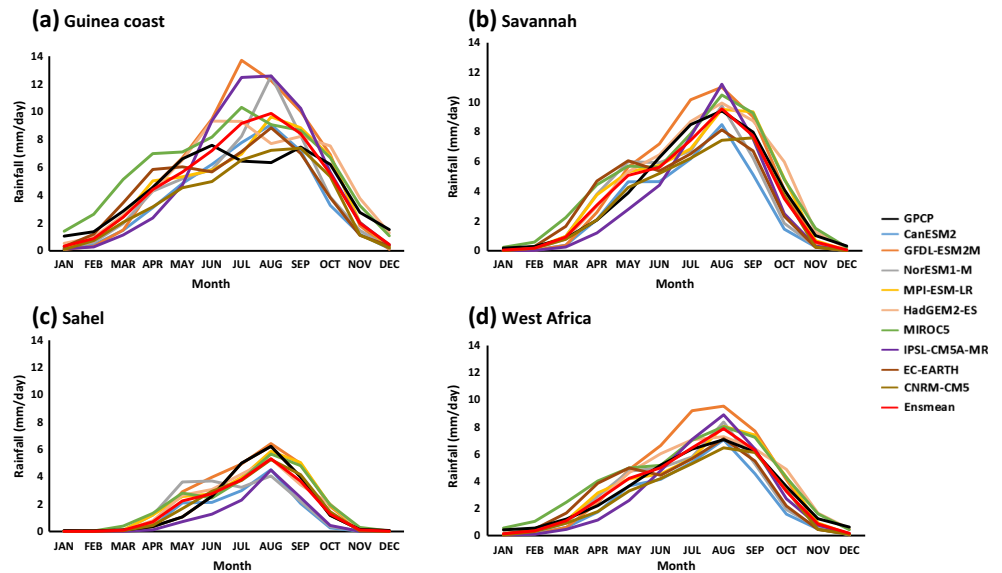
frequency of occurrence of these years compare to GPCP for the study period of 1980–2005, and the results are presented in Fig. 7. The Guinea coast had 17 normal years, 4 dry years, and 5 wet years which were perfectly captured by NorESM1-M. The RCA4 simulations driven by HadGEM2-ES and MIROC5 exhibit highest level overestimation in the occurrence of the dry and wet years while the other simulations had differing levels of accuracy including the Ensmean that underestimated normal and wet years. In the Savannah, 20 normal years, respective 2 and 4 years for dry and wet occurrence were observed in the GPCP observation. The HadGem2-ES and MPI-ESM-LR, respectively, had the highest and lowest number of normal year occurrences, while the MPI-ESM-LR and CanESM2 exhibit the highest

occurrence of dry years. Six of the RCA4 simulations overestimated wet year occurrence by a little margin as compared to the GPCP observation. Over the Sahel subregion, most of the simulations exhibited higher number of wet year occurrence compared to 4 years observed in GPCP. The GFDL-ESM2M had replicated accurately the observed classification with 18 normal, 4 wet, and 4 dry years thus giving the best representation. MIROC5- and CNRM-CM5-driven simulations overestimated the normal years by a value of 1 with the latter also having the lowest count for number of wet years at 3. The Ensmean overestimated the occurrence of wet and dry years.

In the entire West Africa domain, MIROC5, GFDL-ESM2M, NorESM1-M, EC-EARTH, and IPSL-CM5A-MR

Fig. 6 Percentage difference in interannual rainfall over West Africa from 1980 to 2005 for **a** Guinea coast, **b** Savannah, **c** Sahel, and **d** whole West Africa
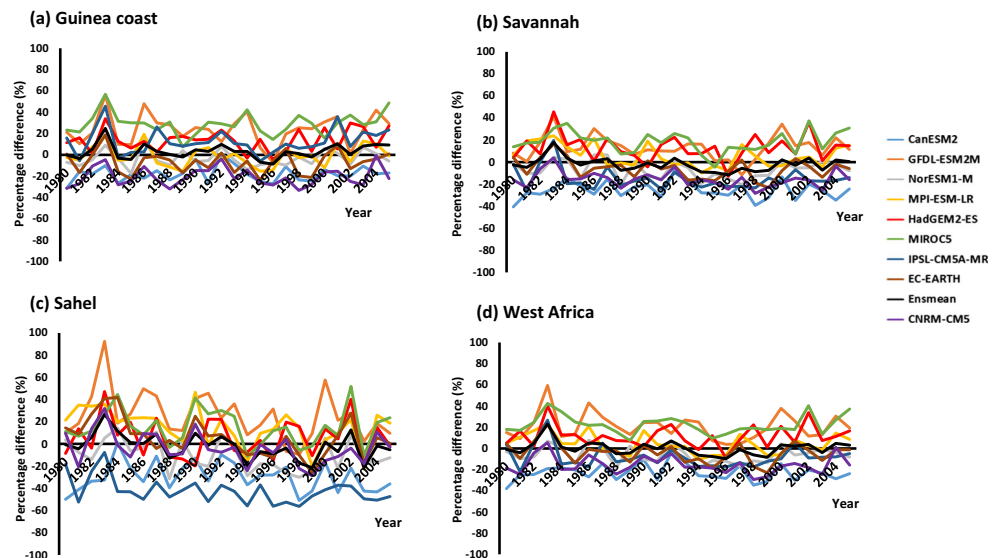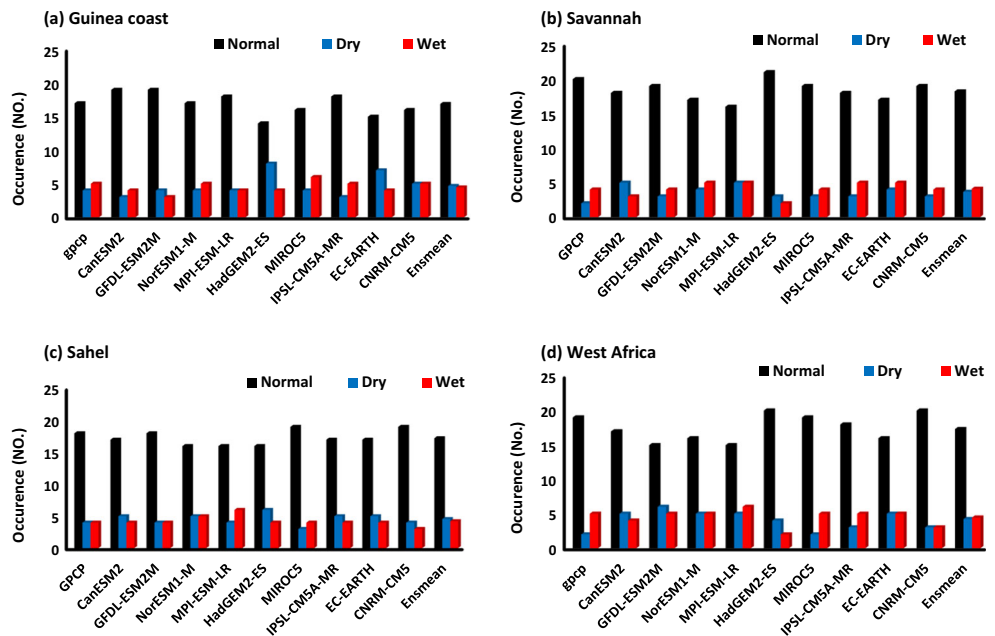
Fig. 7 Occurrence of normal, dry, and wet years between 1980 and 2005 based on the estimated anomalies of annual rainfall amount for **a** Guinea coast, **b** Savannah, **c** Sahel, and **d** whole West Africa


simulated five occurrences of wet years as observed in the GPCP. However, only MIROC5 simulated 19 normal years and 2 dry years which is a perfect replica of the GPCP observation. This observed variability in the RCA4 performance may be associated with large-scale forcing which drives the local climatic conditions (Akinsanola et al. 2015). Depending on the purpose of application and the specific region of concern, it is advised that selecting the appropriate RCA4 member for use should be carefully done in order to yield increased efficiency and effectiveness. Finally, the Ensmean results did not outperform the individual RCA simulation in capturing the normal, dry, and wet year occurrences.

4.4 Statistical analysis

4.4.1 Cumulative density function

The cumulative density function for rainfall amount as shown in Fig. 8a–d offers details on the frequency of occurrence of rainfall amounts in mm/day. For the Guinea coast illustrated in Fig. 8a, most of the RCA4 simulations showed slight overestimations of lower rainfall amounts (between 1 and 3 mm/day) and underestimations for higher amounts (between 8 and 11 mm/day). The GPCP most occurring rainfall amount was 7 mm/day with the MIROC5 been the only simulation to

Fig. 8 The cumulative distribution function of monthly mean rainfall amounts from observations and various model simulations for **a** Guinea coast, **b** Savannah, **c** Sahel, and **d** whole West Africa
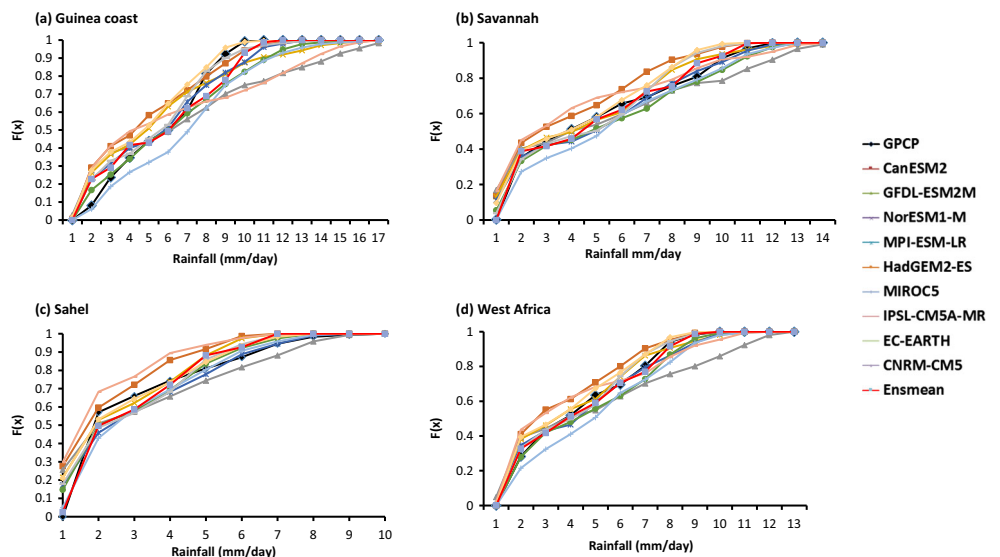
replicate exactly the same trend although with differing margin. Majority of the simulations reported maximum frequency of occurrence between 2 and 6 mm/day as depicted by the gradients of the cumulative distribution curve. The trend in the Savannah also showed higher probabilities of lower rainfall amounts relative to the GPCP as seen in Fig. 8b. The Ensmean captured more effectively the overall trend presented although with some variations while all the other simulations gave slightly more frequent 1–3 mm/day rainfall amounts than observed. All simulations converged at unity (i.e. 1) before or on 14 mm/day, thus eliminating the occurrence of rainfall greater than 14 mm/day. In the Sahel subregion, the Ensmean and MIROC5 replicate more accurately the GPCP frequency of rainfall less than 1 mm/day while the others simulations showed higher frequencies for the same amount. This trend is reversed when rainfall increased to 2 mm/day with the cumulative curves for all the simulations except CanESM2 and IPSL-CM5A-MR been located below that of the GPCP as observed in Fig. 8c. Ultimately, RCA4 simulations driven by CanESM2, IPSL-CM5A-MR, and NorESM1-M all approached unity at about 6–7 mm/day rainfall amount which is below the GPCP maximum of about 9–10 mm/day. Over the larger West Africa domain, the RCA4 simulations presented in Fig. 8d also show a steep gradient around the 1 to 2 mm/day range. The MIROC5 curve is clearly below that of GPCP until around 6 mm/day where it starts to rise, while the GFDL-ESM2M at about the same amount begins to deviate more from the GPCP. All the RCA4 simulations had varying degrees of accuracy with the Ensmean providing the best fit.

4.4.2 Trend detection

The results of the nonparametric Mann-Kendall test used to investigate the presence of significant trends in annual rainfall data is presented in Table 2. Over the Guinea coast and Savannah subregions, GPCP exhibits no significant trend in the annual rainfall series. The null hypothesis is accepted at 95% confidence interval. With respect to the observed dataset, no significant trend was observed in all the RCA4 simulations except in the Savannah where the Ensmean exhibited a significant increasing trend in the annual rainfall series. Furthermore, over the Sahel, GPCP captured a significant increasing trend in annual rainfall series. Only the multimodel ensemble mean and MIROC5 replicated the observation over this subregion. In West Africa, the observation exhibits no significant trend in the annual rainfall series. The majority of the RCA4 simulations were consistent with the observation with differing level of accuracy.

4.4.3 Statistical validation

Several statistical approaches were used to assess the model ability in replicating the rainfall characteristics over the different homogenous subregion and the whole of West Africa domain. The result of the statistics is presented in Tables 3 and 4. The results shown are based on the interannual variation of seasonal mean rainfall for the period 1980–2005. Each RCA4 was compared against the GPCP using MBE, MGE, RMSE, and Pearson's correlation coefficient. The suitability of RCA4 simulations driven by nine CMIP5 GCMs presented here is not only based on the low MBE, MGE, and RMSE but also on positively high correlation value. Over the Guinea coast and in the Savannah subregions during the dry months (DJF), the majority of the RCA4 simulations were not suitable, with only HadGEM2-ES and IPSL-CM5A-MR been suitable. In the Sahel, simulations driven by HadGEM2-ES and EC-EARTH was found to be more suitable over the region, while over the whole of West Africa domain, only HadGEM2-ES and IPSL-CM5A-MR were found to be suitable. The results presented here have clearly shown that the RCA4 simulation driven

Table 2 Result of Mann-Kendall test

Data	Guinea coast Z-value	Savannah Z-value	Sahel Z-value	West Africa Z-value
GPCP	−1.41	1.81	2.56*	1.10
HadGEM2-ES	0.44	0.66	1.81	1.06
MIROC5	0.26	1.96	2.87*	1.54
EC-EARTH	−0.46	−0.57	−0.79	−0.79
MPI-ESM-LR	−0.18	−0.84	0.00	−0.26
NorESM1-M-LR	0.31	0.62	0.66	0.31
CNRM-CM5	−0.13	−0.04	0.00	−0.04
IPSL-CM5A-MR	0.40	−0.13	−0.07	0.04
CanESM2	0.09	0.88	0.66	0.79
GFDL-ESM2M	0.18	1.01	0.40	0.09
Ensmean	0.84	2.05*	2.60[a]	1.98

Negative (positive) Z-value indicates decreasing (increasing) trend

[*] Significant trend at 95% confidence interval

Table 3 Detailed output of the statistical analysis of the RCA for the months of DJF over Guinea coast, Savannah, Sahel and the whole West Africa

Guinea DJF

Model	MBE	MGE	RMSE	r	Remark	MBE	MGE	RMSE	r	Remark
										Savannah DJF
HadGEM2-ES	−0.39	0.39	0.40	0.99	Most suitable	−0.15	0.15	0.15	0.97	Most suitable
MIROC5	0.39	0.69	0.80	−0.01	Not suitable	0.09	0.14	0.18	0.36	Not suitable
EC-EARTH	−0.70	0.70	0.82	0.25	Not suitable	−0.15	0.15	0.19	0.34	Not suitable
MPI-ESM-LR	−0.91	0.91	0.95	0.35	Not suitable	−0.18	0.18	0.19	0.43	Not suitable
NorESM1-M	−0.97	0.97	1.01	0.04	Not suitable	−0.22	0.22	0.23	0.21	Not suitable
CNRM-CM5	−0.97	0.97	1.01	0.37	Not suitable	−0.21	0.21	0.22	0.35	Not suitable
IPSL-CM5A-MR	−1.04	1.04	1.04	0.98	Suitable	−0.25	0.25	0.26	0.53	Suitable
CanESM2	−1.08	1.08	1.10	0.30	Not suitable	−0.24	0.24	0.25	0.15	Not suitable
GFDL-ESM2M	−1.14	1.14	1.16	0.25	Not suitable	−0.25	0.25	0.26	0.21	Not suitable
Ensmean	−0.68	0.68	0.72	0.41	Not suitable	−0.16	0.16	0.17	0.45	Not suitable

Sahel DJF

Model	MBE	MGE	RMSE	r	Remark	MBE	MGE	RMSE	r	Remark
										West Africa DJF
HadGEM2-ES	−0.04	0.04	0.04	0.90	Suitable	−0.18	0.18	0.19	0.99	Most suitable
MIROC5	−0.02	0.02	0.02	−0.57	Not suitable	0.15	0.27	0.31	0.00	Not suitable
EC-EARTH	0.00	0.00	0.00	1.00	Most suitable	−0.29	0.29	0.34	0.22	Not suitable
MPI-ESM-LR	−0.05	0.05	0.05	−0.34	Not suitable	−0.37	0.37	0.39	0.33	Not suitable
NorESM1-M	−0.05	0.05	0.05	−0.89	Not suitable	−0.40	0.40	0.42	0.03	Not suitable
CNRM-CM5	−0.05	0.05	0.05	−0.91	Not suitable	−0.40	0.40	0.42	0.32	Not suitable
IPSL-CM5A-MR	−0.05	0.05	0.05	−0.77	Not suitable	−0.44	0.44	0.44	0.99	Suitable
CanESM2	−0.05	0.05	0.05	−0.97	Not suitable	−0.45	0.45	0.45	0.26	Not suitable
GFDL-ESM2M	−0.05	0.05	0.05	−0.85	Not suitable	−0.47	0.47	0.48	0.22	Not suitable
Ensmean	−0.04	0.04	0.05	−0.28	Not suitable	−0.29	0.29	0.30	0.38	Not suitable

Table 4 Detailed output of the statistical analysis of the RCA for the months of JJAS over Guinea coast, Savannah, Sahel, and the whole West Africa

Guinea JJAS

Model	MBE	MGE	RMSE	r	Remark	MBE	MGE	RMSE	r	Remark
										Savannah JJAS
HadGEM2-ES	1.69	1.69	1.85	0.28	Not suitable	0.42	0.42	0.48	0.98	Most suitable
MIROC5	2.1	2.1	2.46	−0.78	Not suitable	0.27	0.91	0.95	0.91	Suitable
EC-EARTH	0.21	1.39	1.63	−0.8	Not suitable	−1.36	1.36	1.41	0.95	Suitable
MPI-ESM-LR	0.86	1.74	2.01	−0.42	Not suitable	−0.18	0.91	1.1	0.74	Suitable
NorESM1-M-LR	1.78	2.65	3.38	−0.75	Not suitable	−0.88	1.05	1.26	0.8	Suitable
CNRM-CM5	−0.43	0.91	1.38	−0.45	Not suitable	−1.43	1.43	1.61	0.76	Suitable
IPSL-CM5A-MR	4.2	4.2	4.64	−0.99	Not suitable	−0.33	1.23	1.38	0.97	Suitable
CanESM2	0.6	1.43	1.67	−0.89	Not suitable	−1.93	1.93	2.06	0.88	Suitable
GFDL-ESM2M	4.41	4.41	4.94	−0.93	Not suitable	1.3	1.3	1.34	0.99	Suitable
Ensmean	1.34	1.54	1.85	−0.9	Not suitable	−0.41	0.44	0.57	0.96	Suitable

Sahel JJAS

Model	MBE	MGE	RMSE	r	Remark	MBE	MGE	RMSE	r	Remark
										West Africa JJAS
HadGEM2-ES	−0.45	0.7	0.72	0.96	Suitable	0.22	0.34	0.39	1.0	Suitable
MIROC5	−0.27	0.68	0.79	0.84	Suitable	0.7	0.7	0.79	1.0	Suitable
EC-EARTH	0	0	0	1.0	Most suitable	−0.4	0.44	0.51	0.99	Suitable
MPI-ESM-LR	−0.04	0.66	0.77	0.82	Suitable	0.3	0.82	0.88	0.97	Suitable
NorESM1-M-LR	−1.15	1.71	1.75	0.29	Not suitable	−0.12	0.77	0.85	0.96	Suitable
CNRM-CM5	−0.43	0.7	0.83	0.89	Suitable	−0.53	0.53	0.64	0.99	Suitable
IPSL-CM5A-MR	−1.81	1.81	1.89	0.92	Suitable	0.6	0.78	1.01	0.99	Suitable
CanESM2	0.63	0.66	0.86	0.94	Suitable	−0.74	0.74	0.95	0.97	Suitable
GFDL-ESM2M	−1.52	1.52	1.65	0.89	Suitable	1.61	1.81	2.04	0.99	Suitable
Ensmean	−0.53	0.67	0.78	0.95	Suitable	0.1	0.24	0.33	1.0	Most suitable

HadGEM2-ES is best for dry months' rainfall assessment over the study area. In the summer monsoon months of JJAS, the results over Guinea coast indicate that none of the RCA4 simulations is suitable. In Savannah, Sahel and the entire West African domain, all the RCA4 simulations were found to be suitable except for NorESM1-M which was observed to be unsuitable for Sahel. It is worthy to note that the Ensmean exhibits a remarkable result as compared to the individual RCA4 simulations as shown in Table 4. The results have evidently shown that the performance of the RCA4 simulations is weak in the dry months of DJF over all the regions and also in the summer monsoon months of JJAS over the Guinea coast. In addition, the RCA4 simulations and their multimodel ensemble mean exhibited a better performance over larger domain of West Africa than the homogenous subregions. Based on individual RCA4 simulation performance, HadGEM2-ES consistently outperforms all other RCA4 simulations in all the seasons and over majority of the subregions.

5 Conclusion

This study evaluated the historical rainfall characteristics over West Africa using the Rossby Centre Regional Climate Model–RCA4 driven by nine CMIP5 GCMs. Both statistical and climatological approaches were employed in determining the RCA4 simulations performance over the study area. Results from the spatial distribution showed that all the model simulations and their multimodel ensemble mean captured adequately the West Africa precipitation pattern with differing level of accuracy. Majority of the simulation slightly overestimated the orographic induced rainfall over the Guinean Highlands. These results underline the need to correct the systematic error of the model simulated rainfall amounts before any application. Furthermore, the result from the interseasonal variation showed that all the RCA4 simulations except that of HadGEM2-ES and MIROC5 failed to capture the asymmetric behavior of the rainfall amount between the onset and retreat periods as observed in the GPCP observations. Most importantly, the RCA4-driven simulations are weak over the Guinea coast in terms of representing the basic rainfall chacteristics of the subregion. The interannual rainfall variability showed that the RCA4 simulations were consistent in capturing the observed rainfall pattern with differing level of accuracy. The lowest percentage difference in the model performance was observed over the larger West Africa domain while the highest percentage difference was observed in the Sahel subregion. Most of the results indicated that the RCA4 performance is best over a larger domain of West Africa than the three homogeneous subregions. It is also worthy to note that the multimodel ensemble mean consistently outperforms the individual RCA member owing to its lowest percentage difference in rainfall series over all the subregions and the entire West Africa domain. The RCA4

simulations exhibited a good performance in capturing the observed rainfall distributions in the CDF curves and also showed a remarkable performance in capturing the occurrence of wet, dry, and normal years. The Mann–Kendall test showed no significant statistical trend in annual rainfall either in GPCP observation or in the RCA4 simulations over the entire West African domain. Lastly, the result from the statistical analysis explain that the RCA4 simulations performance varies from one season and subregions to another, implying that no single model simulation is best at all time. However, based on individual model performance, HadGEM2-ES-driven simulation consistently outperformed all other simulations. The use of the multimodel ensemble mean has resulted to improved representation of rainfall characteristics over the study domain. Therefore, this study suggests its use for impact studies in the field of climate change and variability over the region. Although, our observations on this are subject and fully relative to the objective functions selected for the assessment.

References

Abiodun BJ, Adeyewa ZD, Oguntunde PG, Salami AT, Ajayi VO (2012) Modeling the impacts of reforestation on future climate in West Africa. Theor Appl Climatol 110(1–2):77–96

Adler RF, Huffman GJ, Chang A, Ferraro R, Xie P-P, Janowiak J, Rudolf B, Schneider U, Curtis S, Bolvin D, Gruber A, Susskind J, Arkin P, Nelkin E (2003) The version-2 Global Precipitation Climatology Project (GPCP) monthly precipitation analysis (1979–present). J Hydrometeorol 4:1147–1167

Afiesimama EA, Pal JS, Abiodun BJ, Gutowski WJ, Adedoyin A (2006) Simulation of west African monsoon using RegCM3 part I: model validation and interannual variability. Theor Appl Climatol 93:245–261

Akinsanola AA, Ogunjobi KO (2015) Recent homogeneity analysis and long term spatio-temporal rainfall trends in Nigeria. Theor Appl Climatol. doi:10.1007/s00704-015-1701-x

Akinsanola AA, Ogunjobi KO, Gbode IE, Ajayi VO (2015) Assessing the capabilities of three regional climate models over CORDEX Africa in simulating west African summer monsoon precipitation. Adv Meteorol 2015:935431 . doi:10.1155/2015/93543113pages

Akinsanola AA, Ogunjobi KO, Ajayi VO, Adefisan EA, Omotosho JA, Sanogo S (2016) Comparison of five gridded precipitation products at climatological scales over West Africa. Meteorol Atmos Phys. doi: 10.1007/s00703-016-0493-6

Christensen J, Christensen O (2007) A summary of the PRUDENCE model projections of changes in European climate by the end of this century. Clim Chang 81:7–30. doi:10.1007/s10584-006-9210-7

Christensen OB, Christensen JH, Machenhauer B, Botzet M (1998) Very high-resolution regional climate simulations over Scandinavia: present climate. J Clim 11:3204–3229

de la Casa A, Nasello O (2010) Breakpoints in annual rainfall trends in Córdoba. Argentina Atmos Res 95:419–427

de la Casa A, Nasello OB (2012) Low frequency oscillation of rainfall in Córdoba, Argentina, and its relation with solar cycles and cosmic rays. Atmos Res 113:140–146

Dee DP, Coauthors (2011) The ERA-Interim reanalysis: configuration and performance of the data assimilation system. Q J R Meteorol Soc 137:553–597

Diallo I, Sylla MB, Camara M, Gaye AT (2012) Interannual variability of rainfall and circulation features over the Sahel based on multiple regional climate models simulations. Theor Appl Climatol. doi:10.1007/s00704-012-0791-y

Diallo I, Sylla MB, Camara M, Gaye AT (2013) Interannual variability of rainfall and circulation features over the Sahel based on multiple regional climate models simulations. Theor Appl Climatol 113(1–2):351–362

Druyan LM, Feng J, Cook KH, Xue Y, Fulakeza M, Hagos SM, Konaré A, Moufouma-Okia W, Rowell DP, Vizy EK, Ibrah SS (2010) The WAMME regional model intercomparison study. Clim Dynam 35(1):175–192. doi:10.1007/s00382-009-0676-7

Feser F, Rockel B, von Storch H, Winterfeldt J, Zahn M (2011) Regional climate models add value to global model data: a review and selected examples. Bull Am Meteorol Soc 92(9):1181–1192

Fuhrer J, Smith P, Gobiet A (2014) Implications of climate change scenarios for agriculture in alpine regions—a case study in the Swiss Rhone catchment. Sci Total Environ 493:1232–1241. doi:10.1016/j.scitotenv.2013.06.038

Gbobaniyi E, Sarr A, Sylla MB, Diallo I et al (2013) Climatology, annual cycle and interannual variability of precipitation and temperature in CORDEX simulations over West Africa. Int J Climatol. doi:10.1002/joc.3834

Giorgi F, Jones C, Asrar G (2009) Addressing climate information needs at the regional level: the CORDEX framework. World Meteorol Organ (WMO) Bull 58(July):175–183

IPCC-TGICA, (2007) General guidelines on the use of scenario data for climate impact and adaptation assessment (version 2). Intergovernmental Panel on Climate Change, Task Group on Data Scenario Support for Impact and Climate Assessment, 66 pp. [Available online athttp://www.ipcc-data.org/guidelines/.]

Jacob D, Coauthors (2014) EURO-CORDEX: new high resolution climate change projections for European impact research. Reg Environ Chang 14:563–578. doi:10.1007/s10113-013-0499-2

Jacob D, Bärring L, Christensen OB, Christensen JH, de Castro M, Déqué M, Giorgi F, Hagemann S, Lenderink G, Rockel B, Sanchez E, Schär C, Seneviratne SI, Somot S, van Ulden A, van den Hurk B (2007) An inter-comparison of regional climate models for Europe: model performance in present-day climate. Clim Chang 81:31–52

Kendall MG (1975) Rank correlation methods. Charles Graffin, London

Kim J, Waliser DE, Mattmann CA, Goodale CE, Hart AF, Zimdars PA, Crichton DJ, Jones C, Nikulin G, Hewitson B, Jack C, Lennard C, Favre A (2014) Evaluation of the CORDEX-Africa multi-RCM hindcast: systematic model errors. Clim Dyn:1189–1202. doi:10.1007/s00382-013-1751-7

Kjellström E, Abrahamsson R, Boberg P, Jernbäcker E, Karlberg M, Morel J, et al. (2014) Uppdatering av det klimatvetenskapliga kunskapsläget. Klimatologi 9. SMHI, SE-60176 Norrköping, Sweden. 65pp (in Swedish)

Klutse NAB, Sylla MB, Diallo I, Sarr A, Dosio A, Diedhiou A, Kamga A, Lamptey B, Ali A, Gbobaniyi EO, Owusu K, Lennard C, Hewitson B, Nikulin G, Panitz H, Buchner M (2015) Daily characteristics of West African monsoon rainfall in CORDEX regional climate models. Theor Appl Climatol. doi:10.1007/s00704-014-1352-3

Krishnakumar KN, Prasada Rao GSHV, Gopakumar CS (2009) Rainfall trends in twentieth century over Kerala. India Atmos Environ 43:1940–1944

Laprise R, Hernández-Díaz L, Tete K, Sushama L, Šeparović' L, Martynov A, Winger K, Valin M (2013) Climate projections over CORDEX Africa domain using the fifth-generation Canadian regional climate model (CRCM5). Clim Dynam 41:3219–3246. doi:10.1007/s00382-012-1651-2

Mann HB (1945) Nonparametric tests against trend. Econometrica 13:245–259

McKee TB, Doesken NJ, Kleist J (1993) The relationship of drought frequency and duration to time scales. Preprints, 8th Conference on Applied Climatology, Anaheim, California, pp 179–184

Nicholson SE (2003) Comments on "The south Indian convergence zone and interannual rainfall variability over south Africa" and the question of ENSO's influence on Southern Africa. J Clim 6:1463–1466

Nikulin G, Jones C, Giorgi F, Asrar G, Buchner M, Cerezo-Mota R, Christensen OB, Deque M, Fernandez J, Hansler A, van Meijgaard E, Samuelsson P, Sylla MB, Sushama L (2012) Precipitation climatology in an ensemble of CORDEX-Africa regional climate simulations. J Climate 25(18):6057–6078. doi:10.1175/JCLI-D-11-00375.1

Omotosho JB, Abiodun BJ (2007) A numerical study of moisture build-up and rainfall over West Africa. Meteorol Appl 14:209–225

Paeth H, Hall NM, Gaertner MA, Alonso MD, Moumouni S, Polcher J, Ruti PM, Fink AH, Gosset M, Lebel T, Gaye AT, Rowell DP, Moufouma-Okia W, Jacob D, Rockel B, Giorgi F, Rummukainen M (2011) Progress in regional downscaling of west African precipitation. Atmos Sci Lett 12(1):75–82

Rummukainen M (2010) State-of-the-art with regional climate models. Wiley Interdiscip. Rev. Climate Change 1:82–96. doi:10.1002/wcc.8

Ruti PM, Williams JE, Hourdin F, Guichard F, Boone A, Van Velthoven P, Favot F, Musat I, Rummukainen M, Dominguez M, Gaertner MA, Lafore JP, Losada T, Rodriguez de Fonseca MB, Polcher J, Giorgi F, Xue Y, Bouarar I, Law K, Josse B, Barret B, Yang X, Mari C, Traore AK (2011) The West African climate system: a review of the AMMA model inter-comparison initiatives. Atmos Sci Lett 12:116–122. doi:10.1002/asl.305

Samuelsson P, Jones CG, Willén U, Ullerstig A, Gollvik S, Hansson U, Hansson U, Jansson C, Kjellströ E, Nikulin G, Wyser K (2011) The Rossby Centre regional climate model RCA3: model description and performance. Tellus A 63:4–23. doi:10.1111/j.1600-0870.2010.00478.x

Stoffel M, Mendlik T, Schneuwly-Bollschweiler M, Gobiet A (2014) Possible impacts of climate change on debris-flow activity in the Swiss Alps. Clim Chang 122:141–155. doi:10.1007/s10584-013-0993-z

Strandberg G, Bärring L, Hansson U, Jansson C, Jones C, Kjellström E, Kolax M, Kupiainen M, Nikulin G, Samuelsson P et al (2014) CORDEX scenarios for Europe from the Rossby. Centre regional climate model RCA4; report meteorology and climatology no. 116. Swedish Meteorological and Hydrological Institute, Norrköping, Sweden

Subash N, Singh SS, Priya N (2011) Variability of rainfall and effective onset and length of the monsoon season over a sub-humid climatic environment. Atmos Res 99:479–487

Sultan B, Janicot S (2000) Abrupt shift of the ITCZ over West Africa and intra-seasonal variability. Geophys Res Lett 27:3353–3356. doi:10.1029/1999GL011285

Sylla M, Giorgi R, Ruti M, Calmanti S, Dell'Aquila A (2011) The impact of deep convection on the west African summer monsoon climate: a regional climate model sensitivity study. Q J R Meteorol Soc 137:1417–1430. doi:10.1002/qj.853

Sylla MB, Diallo I, Pal JS, (2013) West African monsoon in state-of-the-art regional climate models. In Tarhule A (ed) Climate variability—regional and thematic patterns

Taylor KE, Stouffer RJ, Meehl GA (2012) An overview of CMIP5 and the experiment design. Bull Am Meteor Soc 93:485–498

Udo RK (1978) A comprehensive geography of West Africa. Heinemann Educational Books, London, pp 1–50

van der Linden P, Mitchell J, Eds, (2009) ENSEMBLES: climate change and its impacts: summary of research and results from the ENSEMBLES project. Met Office Hadley Centre, 160 pp

Xue Y, Lau K-M, Cook KH, Rowell DP, Boone A, Feng J, Konare A, De Sales F, Bruecher T, Dirmeyer P, Druyan LM, Fulakeza M, Guo Z, Hagos SM, Kim K-M, Kitoh A, Kumar V, Lonergan P, Pasqui M, Poccard-Leclercq I, Mahowald N, Moufouma-Okia W, Pegion P, Sanda IS, Schubert SD, Sealy A, Thiaw WM, Vintzileos A, Vizy EK, Williams S, Wu M-LC (2010) Intercomparison and analyses of the West African monsoon and its variability in the West African monsoon modelling and evaluation project (WAMME) first model inter-comparison experiment. Clim Dyn 35:3–27. doi:10.1007/s00382-010-0778-2

Xue Y, Janjic Z, Dudhia J, Vasic R, De Sales F (2014) A review on regional dynamical downscaling in intraseasonal to seasonal simulation/prediction and major factors that affect downscaling ability. Atmos Res 147–148:68–85